Nano Research

Open Access

Research Article

A copper-coordinated porous organic polymer catalyst with binuclear bis(imino)pyridine coordination units for promoting de/hydrogenation transformations of diverse carbon nitrogen bonds

Jiawei Zou[1,2], Siyuan Wang[3], Laidong Li[4], Guanglin Wang[5], Jiuxiang Ding[4], Wenzhuo Li[4], Jingyi Su[4], Xuebo Chen[1] ✉, and Wenying Ai[1,4] ✉

[1] College of Chemistry and Molecular Sciences, Henan University, Zhengzhou 450046, China
[2] Jilin City Talent Service Center, No. 166, Liaobu Road, Changyi District, Jilin 132000, China
[3] Zhengzhou Branch of China Nuclear Power Engineering Co., LTD., Zhengzhou 450000, China
[4] School of Materials Electronics and Energy Storage, Zhongyuan University of Technology, Zhengzhou 450007, China
[5] Center of Basic Molecular Science (CBMS), Department of Chemistry, Tsinghua University, Beijing100084, China

Cite this article: *Nano Research*, **2026**, *19*, 94908329. https://doi.org/10.26599/NR.2026.94908329

ABSTRACT: Catalytic hydrogenation/dehydrogenation of carbon nitrogen bonds (–CH–NH–, –C=N–, –C≡N) represents fundamental transformations in synthetic chemistry and hydrogen storage. While significant advances have been made in hydrogenation or dehydrogenation individually, reversible interconversion using a single catalyst remains challenging. To address this challenge, we develop a copper-coordinated porous organic polymer (POP) catalyst featuring binuclear bis(imino)pyridine coordination units (dibis(imino)pyridine). This dibis(imino)pyridine-based POP catalyst could reversibly mediate both the dehydrogenation transformation of benzylamine compounds and the hydrogenation transformations of nitriles. Remarkably, both transformations proceed efficiently under mild conditions (water solvent, ≤ 80 °C) in the absence of precious metals, while demonstrating excellent catalytic recyclability with consistent product yields across successive cycles.

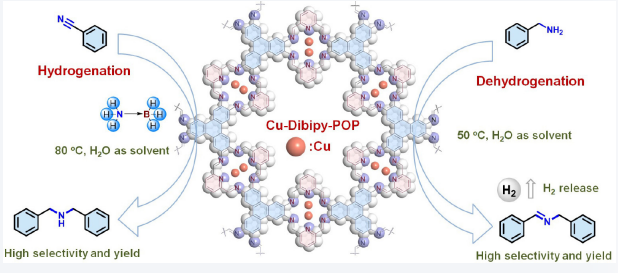

KEYWORDS: hydrogenation, dehydrogenation, dibis(imino)pyridine-based porous organic polymer (POP) catalyst, diverse carbon nitrogen bonds, mild conditions

1 Introduction

Catalytic hydrogenation and dehydrogenation represent pivotal methodologies in organocatalytic systems, serving as indispensable reaction pathways for molecular saturation/desaturation transformations in synthetic chemistry applications [1–3]. Notably, these transformations have garnered significant research interest as enabling mechanisms for molecular hydrogen carrier technologies, specifically through reversible hydrogen fixation via covalent bonding in organic molecules [4–6]. As one of the most ubiquitous bonding motif in organic compounds, carbon nitrogen bonds (–CH–NH–, –C=N–, and –C≡N) have attracted substantial research attention regarding their hydrogenation/dehydrogenation transformations, particularly due to their fundamental role in molecular storage systems and synthetic chemistry applications (Fig. 1(a)) [7–14]. Significant advances in this field have been achieved by several research groups, for example, Zhang's and Voutchkova–Kostal's groups have respectively achieved acceptorless dehydrogenation of amines to valuable imine products through photocatalytic and palladium-catalyzed approaches; in 2024, Ma and co-workers developed an atomically dispersed Rh catalyst, which exhibited very high activity in the hydrogenation reaction of benzonitrile and delivered high selectivity toward secondary amine products, and both cyano group and imine bond hydrogenation are involved in this transformation; moreover, Liu and co-workers fabricated a cobalt-catalyzed chemodivergent transfer hydrogenation system for the selective conversion of nitriles to primary, secondary, and tertiary amines.

Despite significant progress has been made in controlling carbon nitrogen bond hydrogenation or dehydrogenation individually, the development of a single catalyst capable of reversibly mediating both transformations still remains a fundamental challenge. To

Received: July 29, 2025; **Revised:** November 17, 2025
Accepted: December 10, 2025

✉Address correspondence to Wenying Ai, 6786@zut.edu.cn; Xuebo Chen, xuebochen@bnu.edu.cn

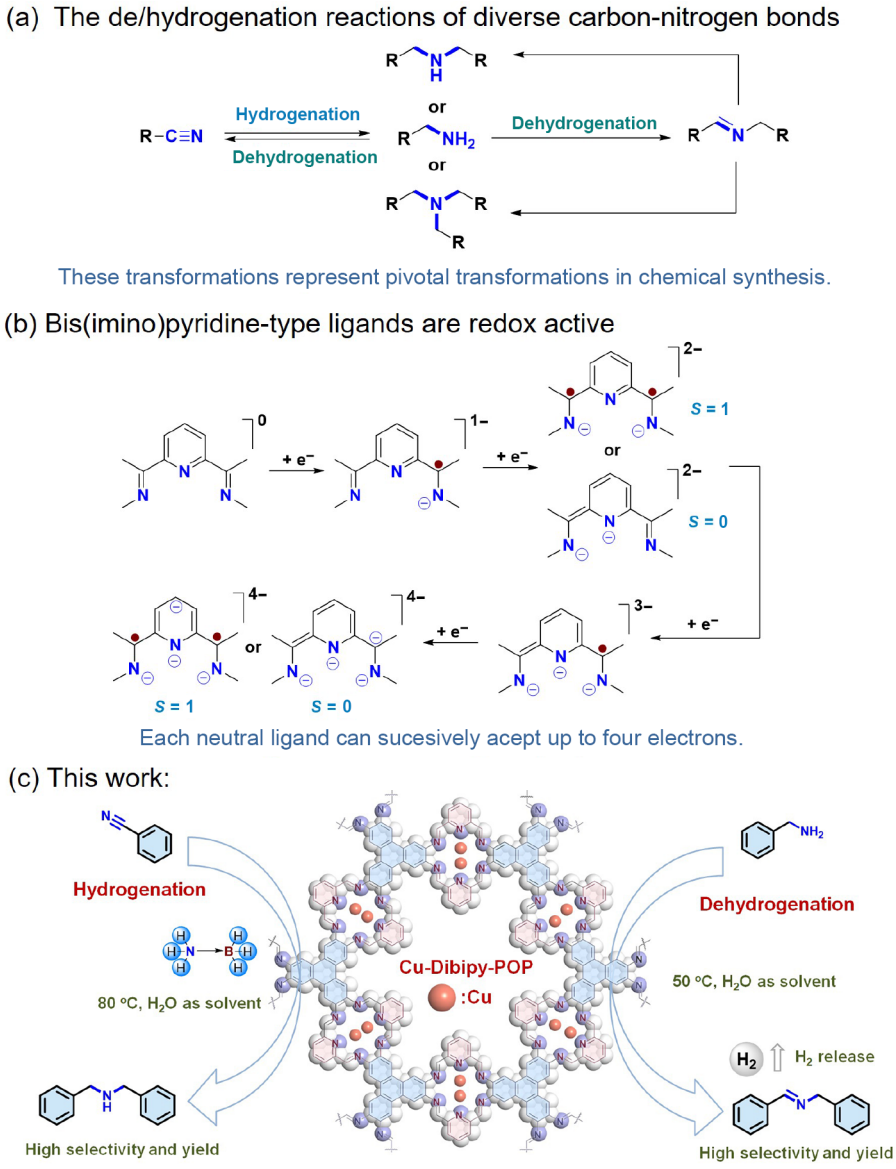

Figure 1 (a) The de/hydrogenation transformations of diverse carbon nitrogen bonds (–CH–NH–, –C=N–, and –C≡N). (b) Bis(imino)pyridine-type ligands are redox active. (c) This work.

address this challenge, the catalyst must possess exceptional hydrogen transfer capability to simultaneously achieve superior catalytic activity [15] in both hydrogenation and dehydrogenation transformations. Current catalytic systems for the de/hydrogenation transformations of carbon nitrogen bonds can be broadly classified into homogeneous and heterogeneous catalysts, each exhibiting distinct characteristics: homogeneous metal complexes offer well-defined active sites, enabling molecular-level mechanistic understanding and precise tunability [16–18], however, their poor recyclability poses significant challenges for industrial-scale applications; heterogeneous catalysts, while more practical for industrial-scale processes, typically contain diverse and structurally complex active sites, moreover, the catalytic centers on the support surface often exist in isolated, disordered configurations, making it difficult to achieve synergistic control over the chemoselectivity of hydrogenation/dehydrogenation products [19–23]. Therefore, the development of novel catalytic systems integrating high selectivity, reversibility, and recyclability for the hydrogenation/dehydrogenation transformations of carbon nitrogen bonds is of great current interest.

Porous organic polymers (POPs), formed through covalent bonding of purely organic building blocks, serve as multifunctional platforms with significant scientific interest [24–29]. More recently, POPs have garnered significant research interest owing to their promising catalytic applications. The flexible design and synthetic tunability of POPs allow for the straightforward incorporation of coordination functional groups into their pores, facilitating precise control over their interactions with metal ions [30]. Therefore, we propose developing a novel POP-based hydrogenation–dehydrogenation catalyst, and enhance its catalytic activity and chemoselectivity through structural modulation of coordination units.

Among the diverse coordination units [31], the bis(imino)pyridine moiety has been extensively validated in coordination chemistry as a well-defined pincer ligand. Previous research has demonstrated that the bis(imino)pyridine complexes

possess remarkable redox catalytic properties due to their distinctive electronic structure and coordinatively unsaturated metal centers [32–35]. The bis(imino)pyridine ligands feature two vacant π*-orbitals that exhibit antibonding character with respect to the imine and pyridine C=N linkages, while simultaneously demonstrating bonding interactions with the C_{imine}–$C_{pyridine}$ connections [36, 37]. Consequently, each neutral bis(imino)pyridine ligand can sequentially accommodate up to four electrons (Fig. 1(b)). Bis(imino)pyridine units exhibited outstanding catalytic performance in numerous homogeneous and heterogeneous systems for hydrogenation, dehydrogenation, and transfer hydrogenation reactions [34, 38]. For instance, our group previously reported a crystalline two-dimensional (2D) nickel-coordinated bis(imino)pyridine-based metal-covalent organic framework (**Ni-bipy-COF**) in 2022 [39], which was shown to effectively catalyze the transfer hydrogenation of quinolines using ammonia borane as the hydrogen donor. Based on literature reports and our group's previous studies, we hypothesize that increasing the density of bis(imino)pyridine within POP skeletons may further enhance the redox activity of the POP framework as a bulky ligand to some extent. This would weaken the bond energy of the catalytic active intermediate metal–hydride species (M–H), facilitating the cleavage of the M–H bond during hydrogen transfer and thereby improving hydrogen transfer efficiency. Consequently, such a modified POP framework may exhibit superior catalytic performance in both hydrogenation and dehydrogenation transformations of diverse carbon nitrogen bonds. To verify this hypothesis, in this work, we elaborately designed and synthesized a novel POP material incorporating binuclear bis(imino)pyridine coordination units (dibis(imino)pyridine), which could serve as a macro-ligand to coordinate with copper ions, and exhibit efficient catalytic activity for the dehydrogenation transformation of benzylamine compounds and the hydrogenation transformations of nitriles. These two reactions totally involved three fundamental C–N bond transformations: (1) C(sp^3)–N bond dehydrogenation, (2) –C=N– double bond hydrogenation, and (3) –C≡N triple bond hydrogenation. Notably, both transformations proceed under mild conditions (≤ 80 °C, water solvent) without noble metals, maintaining comparable yields over multiple cycles.

2 Results and discussion

The dibis(imino)pyridine-linked POP (**Dibipy-POP**) was prepared through the Schiff-condensation between 2,3,6,7,10,11-hexaaminotriphenylene (**1**) and pyridine-2,6-dicarbaldehyde (**2**) (Fig. 2(a)). Under the solvothermal conditions (mesitylene and N-methylpyrrolidone, p-toluenesulfonic acid, 120 °C, 3 days), **Dibipy-POP** material was generated as brownish red powder (73% isolated yield). The resulting **Dibipy-POP** material is insoluble in most common organic solvents and water. The subsequent metallation of **Dibipy-POP** was performed via 72-hour agitation with $Cu(OAc)_2$ in methanol, thereby yielding the Cu-coordinated framework designated as **Cu-Dibipy-POP**. To eliminate residual metal precursors, the resultant material was washed with methanol, followed by vacuum drying at 60 °C to constant mass.

The structural feature of **Dibipy-POP** and **Cu-Dibipy-POP** was characterized by Fourier transform infrared spectroscopy (FT-IR), cross-polarization magic angle spinning carbon-13 nuclear magnetic resonance (CP/MAS ^{13}C NMR) spectroscopy, and powder X-ray diffraction (PXRD). The FT-IR spectra of **Dibipy-POP** showed the appearance of characteristic C=N stretching vibration at 1625 cm^{-1} [40], with diminished absorption bands corresponding to aldehyde carbonyl groups (1717 cm^{-1}) and primary amines (3300 cm^{-1}) (Fig. 2(b)). The introduction of Cu^{2+} ions into the bis(imino)pyridine chelating motifs of the porous organic polymer framework induced an obvious weakened of imine bands at 1625 cm^{-1}, demonstrating the coordination of Cu^{2+} ion by imine.

The CP/MAS ^{13}C NMR spectroscopy of **Dibipy-POP** revealed diagnostic signal of imine carbons at 153 ppm, and the signals near 110, 126 and 141 ppm can be assigned to the C atoms on the phenyl and pyridine rings (Fig. 2(c)). In addition, the CP/MAS ^{13}C

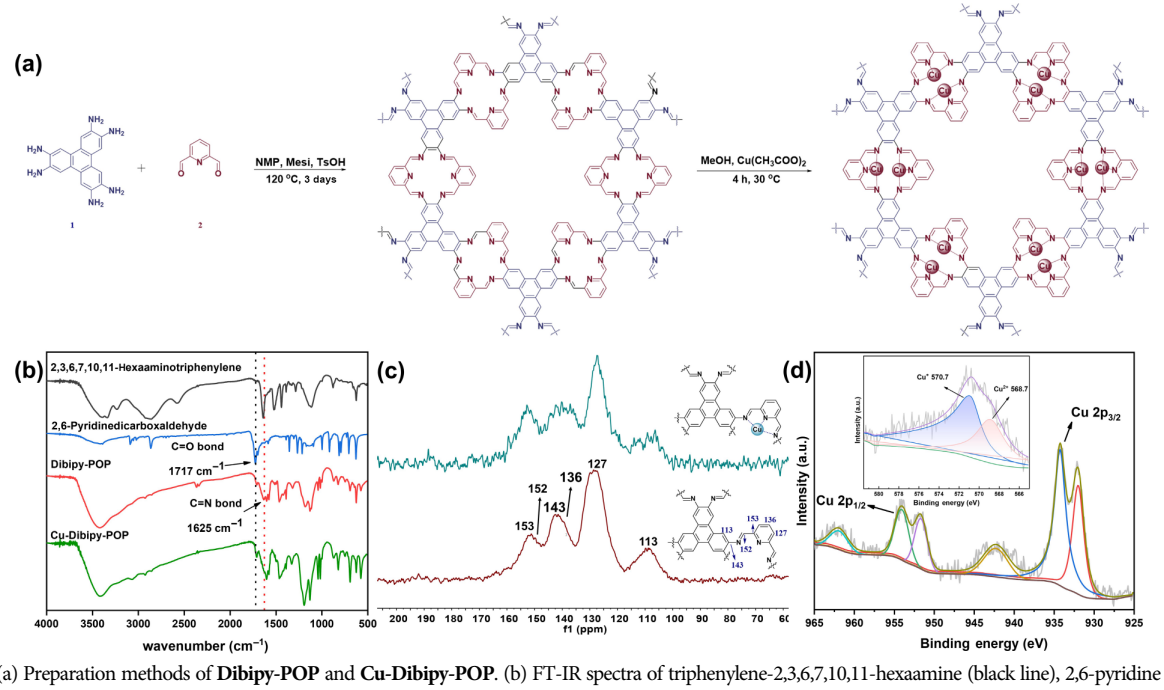

Figure 2 (a) Preparation methods of **Dibipy-POP** and **Cu-Dibipy-POP**. (b) FT-IR spectra of triphenylene-2,3,6,7,10,11-hexaamine (black line), 2,6-pyridine dialdehyde (blue line), **Dibipy-POP** (red line), and **Cu-Dibipy-POP** (green line). (c) The CP/MAS ^{13}C NMR spectra of **Dibipy-POP** (red line) and **Cu-Dibipy-POP** (green line). (d) XPS analysis of the Cu 2p region and LMM (inset) in **Cu-Dibipy-POP**.

NMR spectroscopy of **Cu-Dibipy-POP** retained signal correspondence with **Dibipy-POP** in both aromatic and pyridinic carbon regions, suggesting that post-synthetic modification preserved the original structure (Fig. 2(c)). PXRD measurement showed **Dibipy-POP** and **Cu-Dibipy-POP** were amorphous (Fig. S1 in the Electronic Supplementary Material (ESM)). X-ray photoelectron spectroscopy (XPS) was performed to investigate the oxidation state of Cu species and the interaction of Cu–N. As depicted in Fig. 2(d), XPS analysis displayed Cu $2p_{3/2}$ and $2p_{1/2}$ peaks centered at 934.6 and 954.4 eV, respectively [41], illustrating that the oxidation state of copper species in **Cu-Dibipy-POP** existed in the +2 state. To further confirm the presence of Cu^{+} or Cu^{0} species in **Cu-Dibipy-POP**, the high-resolution Cu LMM spectra was conducted. The binding energy peak at 568.7 eV suggested the presence of Cu^{2+} species, and the peak at 570.7 eV is assigned to Cu^{+}. Notably, no characteristic peak corresponding to Cu^{0} species was observed near 568.0 eV (Fig. 2(d)). These results demonstrate the Cu species in **Cu-Dibipy-POP** were the mixture of Cu^{2+} and Cu^{+}, likely arising from partial reduction of Cu^{2+} during the heating and drying process of the sample. Quantitative analysis revealed that Cu(I) and Cu(II) species account for 37.82% and 62.18% of the total copper content, respectively (Fig. S2 in the ESM).

The high-resolution C 1s peaks were deconvoluted into two peaks, which are assigned to C=N bonds and C=C bonds, corroborating the successful realization of dibis(imino)pyridine structures in **Dibipy-POP** and **Cu-Dibipy-POP** (Fig. S3 in the ESM) [42]. The N 1s XPS spectrum of **Dibipy-POP** can be deconvoluted into two peaks at 398.3 and 399.8 eV [43], corresponding to C=N and pyridinic nitrogen [44]. Compared with **Dibipy-POP**, the N 1s XPS spectrum of **Cu-Dibipy-POP** showed a slight shift to higher binding energy, which can be attributed to the coordination between N atoms and copper (Fig. S4 in the ESM).

Solid-state ultraviolet–visible (UV–Vis) spectroscopy showed a significant red shift in **Cu-Dibipy-POP** relative to **Dibipy-POP**, which can be attributed to the Cu loading (Fig. S5 in the ESM). And the Cu loading content in **Cu-Dibipy-POP** is about 5.2 wt.% as measured by inductively coupled plasma-mass spectrometry (ICP-MS) (Table S3 in the ESM). Then, thermogravimetric analysis (TGA) of these two materials were conducted, and demonstrated that both materials maintained structural integrity at temperatures up to 400 °C under an inert atmosphere, satisfying the fundamental requirements for heterogeneous catalysis (Fig. S6 in the ESM).

Scanning electron microscopy (SEM) was employed to characterize the morphology of the two materials (Fig. S7 in the ESM). Both **Dibipy-POP** and **Cu-Dibipy-POP** all exhibited comparable spherical morphologies at the microscale. Notably, the nanoparticle size of **Cu-Dibipy-POP** was changed compared to that of the parent **Dibipy-POP**, likely due to the coordination effects of copper ions during metalation [45]. Moreover, we utilized aberration-adjusted scanning transmission electron microscopy (HAADF-STEM) and extended X-ray absorption fine structure (EXAFS) to further confirm the proposed bimetallic copper sites in **Cu-Dibipy-POP**. HAADF-STEM image revealed that the Cu atoms were atomically dispersed in pairs within the frameworks, and provided direct evidence for the existence of binuclear copper sites within the **Cu-Dibipy-POP** structure (Fig. S8 in the ESM**).** To gain deeper insights into the coordination environment and oxidation state of copper, EXAFS measurements were performed at the Cu-K edge [46]. The Cu K-edge XANES spectra indicates that that the copper species are predominantly in the +2 oxidation state (Fig. S9(a) in the ESM). The *R*-space spectrum exhibited a prominent peak at approximately 1.5 Å, corresponding to the first coordination shell of Cu–N. Notably, no peak was observed around 2.2 Å, indicating the absence of Cu–Cu bond (Fig. S9(b) in the ESM). EXAFS fitting analysis further revealed that the Cu centers are coordinated by three nitrogen atoms, which confirmed the existence of copper-coordinated binuclear bis(imino)pyridine units. In addition, TEM characterization of **Cu-Dibipy-POP** was also performed to verify the discrete nature and distribution of the copper catalytic sites (Fig. S10 in the ESM). TEM image clearly showed the absence of copper clusters in the porous material. This fact, combined with the HAADF-STEM characterization, collectively demonstrates that the copper species exist in a dispersed state within the framework.

The elemental distributions of C, N, O, and Cu within the **Cu-Dibipy-POP** material were analyzed using energy-dispersive X-ray spectroscopy (EDS) elemental mapping (Fig. S11 in the ESM). The EDS mapping results confirm a homogeneous spatial distribution of all elements and highlight their essential contribution to the structural stability of the **Cu-Dibipy-POP**. In addition, elemental analysis was conducted to determine the chemical composition of the material (Table S4 in the ESM).

Subsequently, N_2 adsorption was performed at 77 K to evaluate the permanent porosity of **Dibipy-POP** and **Cu-Dibipy-POP** (Figs. S12(a) and S12(b) in the ESM). The Brunauer–Emmett–Teller (BET) surface areas of **Dibipy-POP** and **Cu-Dibipy-POP** were calculated to be 20 and 34 $m^2 \cdot g^{-1}$, respectively. Unfortunately, the surface area values of these two POPs were very low, which may be attributed to their disordered amorphous structures. And the metal-loaded material exhibited a slight increase in specific surface area compared to the pristine sample, likely due to minor structural disintegration induced during the metal loading process, which contributed to this slight enhancement. The pore sizes of the two POPs were analyzed using the non-local density functional theory (NLDFT) model, and both were determined to be 1.70 nm (Figs. S12(c) and S12(d) in the ESM). While theoretically, the low specific surface area and small pore size would hinder reactant mass transport and potentially impact reaction efficiency, the unique dibis(imino)pyridine coordination units in this material are anticipated to significantly enhance the surface catalytic efficiency, thereby mitigating the limitations imposed by the low surface area. Based on this hypothesis, subsequent evaluation of the catalytic performance of **Cu-Dibipy-POP** included specifically designed control experiments to investigate whether its low specific surface area would adversely affect the catalytic efficiency. The results demonstrated that despite the relatively low surface area, the material exhibited remarkable catalytic activity. Detailed experimental procedures are provided in the final section of the performance study.

2.1 Cu-Dibipy-POP-catalyzed reduction transformation of arene nitriles

The hydrogenation of nitrile compounds offers an environmentally friendly, streamlined one-step approach to producing high-value amine products [17]. However, this transformation faces significant selectivity challenges due to the concurrent generation of diverse amine species, including primary, secondary, tertiary amines as well as imine byproducts (Fig. 3) [47]. Especially for secondary amine formation, controlling product selectivity poses major synthetic

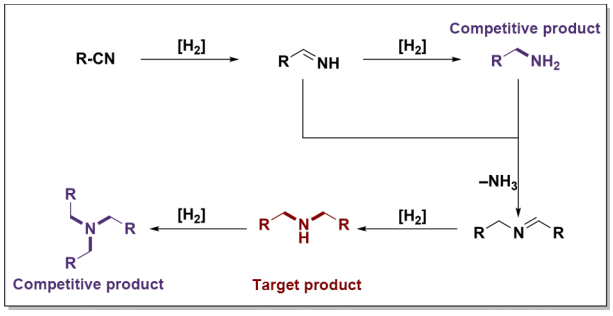

Figure 3 Possible reaction pathways for the hydrogenation transformation of nitriles.

challenge. The complexity arises from the multi-step mechanism required for nitrile-to-secondary-amine conversion, which involves no fewer than four distinct reaction stages. Meanwhile, excessive transamination-reduction leading to tertiary amine formation must be prevented. In addition, symmetrical diamines, particularly those with symmetric structures, serve as crucial chemical intermediates. Their unique molecular architecture and reactive properties make them indispensable in pharmaceutical development, agrochemical synthesis, and the construction of functional materials [48–52]. Consequently, developing a broadly applicable chemoselective route to secondary amines through nitrile hydrogenation represents a critical challenge in organic synthesis [53–55].

Traditional nitrile reduction employs stoichiometric and sensitive hydride reagents, which exhibit low atom economy and limited functional group compatibility. Clearly, employing catalytic hydrogenation for nitriles affords a more sustainable synthetic pathway. Two distinct catalytic approaches for these reductions are direct reduction using H_2 gas and transfer hydrogenation. These transformations involve different hydrogen sources, such as H_2 [56], sodium borohydride ($NaBH_4$) [57], and ammonia-borane (AB, NH_3-BH_3) [39]. Among these different hydrogen sources, AB stands out as a promising hydrogen donor due to its substantial 19.6 wt.% hydrogen content, low toxicity, enhanced operational safety, and remarkable stability. Consequently, herein, AB was selected as the hydrogen source to evaluate the performance of **Cu-Dibipy-POP** in facilitating nitrile reduction reactions.

After the optimized reaction conditions were established, the scope of the catalytic system was explored using various benzonitrile compounds. The **Cu-Dibipy-POP** catalyst exhibited excellent substrate applicability, and benzonitriles bearing both electron-withdrawing and electron-donating groups were transformed into the corresponding secondary amines in good yields (Fig. 4). Notably, substrate with strongly coordinating amino group was also efficiently converted to target product (3e).

The recyclability and durability of **Cu-Dibipy-POP** were examined in the hydrogenation of benzonitrile to evaluate its practicability (Fig. S13 in the ESM). The results demonstrated that the **Cu-Dibipy-POP** catalyst could be reused for at least five consecutive reaction runs without significant loss of catalytic activity or selectivity, and the catalyst could be easily recycled via centrifugation. The FT-IR and XPS analyses of **Cu-Dibipy-POP** after the catalytic hydrogenation have been performed (Figs. S14 and S15 in the ESM). The FT-IR results suggested that the structure of **Cu-Dibipy-POP** remains intact without significant changes after catalytic reactions. XPS analysis revealed that the valence state distribution of copper ions in the **Cu-Dibipy-POP** catalyst remained largely unchanged after the hydrogenation of benzonitrile.

To explore whether the reaction proceeds via a direct hydrogenation or a transfer hydrogenation mechanism, we established a dual-catalytic system for mechanistic studies. Specifically, NH_3BH_3 was subjected to dehydrogenation catalyzed by **Cu-Dibipy-POP** in one reaction vessel, which was connected via a gas-permeable tube to a secondary flask containing 2-vinylnaphthalene and Pd/C dispersed in toluene. The hydrogenation product, 2-ethylnaphthalene, was isolated in 86% yield, confirming the release of molecular hydrogen during the **Cu-Dibipy-POP**-catalyzed dehydrogenation of NH_3BH_3 (Fig. S16(a) in the ESM) [10, 58].

And then, to investigate the influence of the catalyst, we performed the following experiments: (1) When the reactions were conducted without catalyst or only using **Dibipy-POP** as catalyst

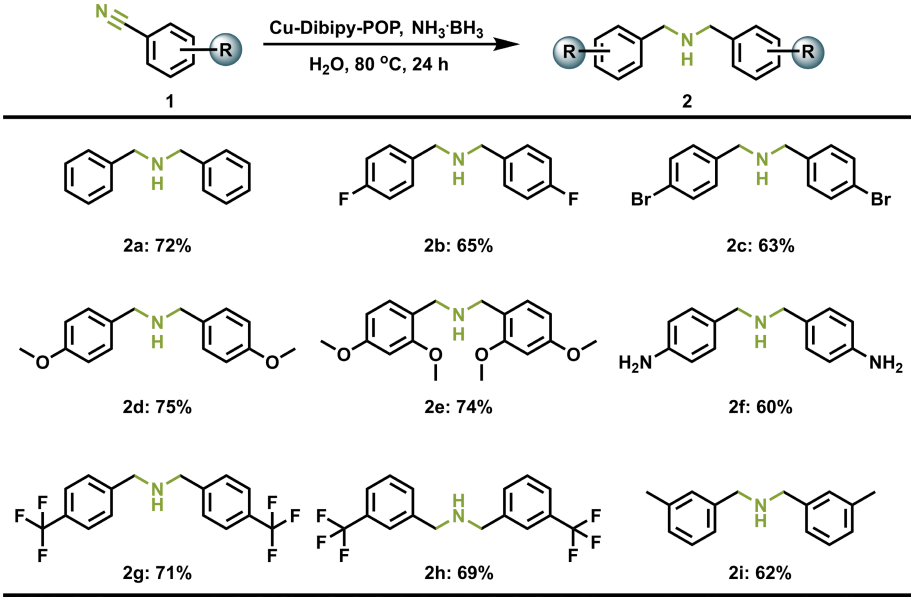

Figure 4 **Cu-Dibipy-POP**-catalyzed hydrogenation of benzonitrile. Reaction conditions: benzonitrile (50 μL, 1 eq.), AB (45 mg, 3 eq.), **Cu-Dibipy-POP** (50 mg), solvent (5 mL), 80 °C, 24 h.

(Figs. S16(b) and S16(c) in the ESM), there were no target dibenzylamine products detected after 24 h; (2) when copper acetate ($Cu(OAc)_2$) was employed as the catalyst, the product yield reached only 6% (Fig. S16(d) in the ESM). These results clearly demonstrate that the metal active center and the ligand cooperate synergistically in catalyzing this transformation, and neither can be omitted.

Finally, to further verify the catalytic mechanism of the reaction pathway, we rigorously excluded potential hydrolysis-hydrogenation routes: (1) Under standard conditions without the hydrogen source (AB), neither dibenzylamine nor its potential precursor (benzamide) was detected (Fig. S16(e) in the ESM). (2) Parallel experiments using benzamide as the direct substrate confirmed that benzamide could not be converted into dibenzylamine derivatives in this catalytic system (Fig. S16(f) in the ESM).

These results definitively confirm that the catalytic system proceeds via direct consecutive hydrogenation of the nitrile group (–CN) to form the target products, rather than through a stepwise conversion involving amide intermediates. This mechanistic investigation provides critical experimental evidence for understanding the unique activity of **Cu-Dibipy-POP** catalysts in the selective hydrogenation of nitrile compounds.

Given the presence of copper ions in two distinct oxidation states within the **Cu-Dibipy-POP** catalyst, control experiments were designed to elucidate whether Cu(I) or Cu(II) species play the pivotal role in the catalytic reaction. Therefore, we performed control experiments for the hydrogenation of benzonitrile by using CuOAc and $Cu(OAc)_2$ as catalysts, respectively. As shown in Figs. S21(a) and S21(b) in the ESM, CuOAc afforded significantly higher yield than $Cu(OAc)_2$ in this catalytic system. These results clearly demonstrate that Cu(I) species plays a more critical role in the catalytic hydrogenation. Notably, the incorporated dibis(imino)pyridine unit serves as a highly redox-active site. It could accept electrons during the catalytic cycle to stabilize low-valent copper active species, thus enabling the superior performance of the catalyst.

Based on these experimental results, we proposed a presumable mechanism (Fig. 5). Initially, **Cu-Dibipy-POP** could react with AB to release Cu–H species [Cu-1] and NH_2BH_2. Then benzonitrile will be reduced by Cu–H via a six-membered ring transition state ([Cu-2]), and gave intermediate [Cu-3]. Subsequently, a benzylimine intermediate could be generated from [Cu-3] through a ligand dissociation step. Within the second catalytic cycle, benzylimine will be reduced by Cu–H species through another six-membered transition state [Cu-4]. This transition state will release the benzylamine molecule via the [Cu-5] intermediate. Next, the benzylamine generated in this step will react with benzylimine intermediate through a condensation step in the system, producing the N-benzylideneaniline intermediate. And this benzylideneaniline intermediate will undergo another hydrogenation process, fully reducing the C=N bond to form dibenzylamine product.

2.2 Cu-Dibipy-POP-catalyzed dehydrogenation of benzylamine

Imine compounds are a versatile class of chemical intermediates with significant importance in agricultural, pharmaceutical, and synthetic chemistry [59]. Especially, symmetrical imines usually act as crucial intermediates in the synthesis of natural products, or as as a precursor for the preparation of small molecules of biomedical relevance [60–62]. Among the numerous approaches to synthesizing imines, the dehydrogenation of benzylamine has

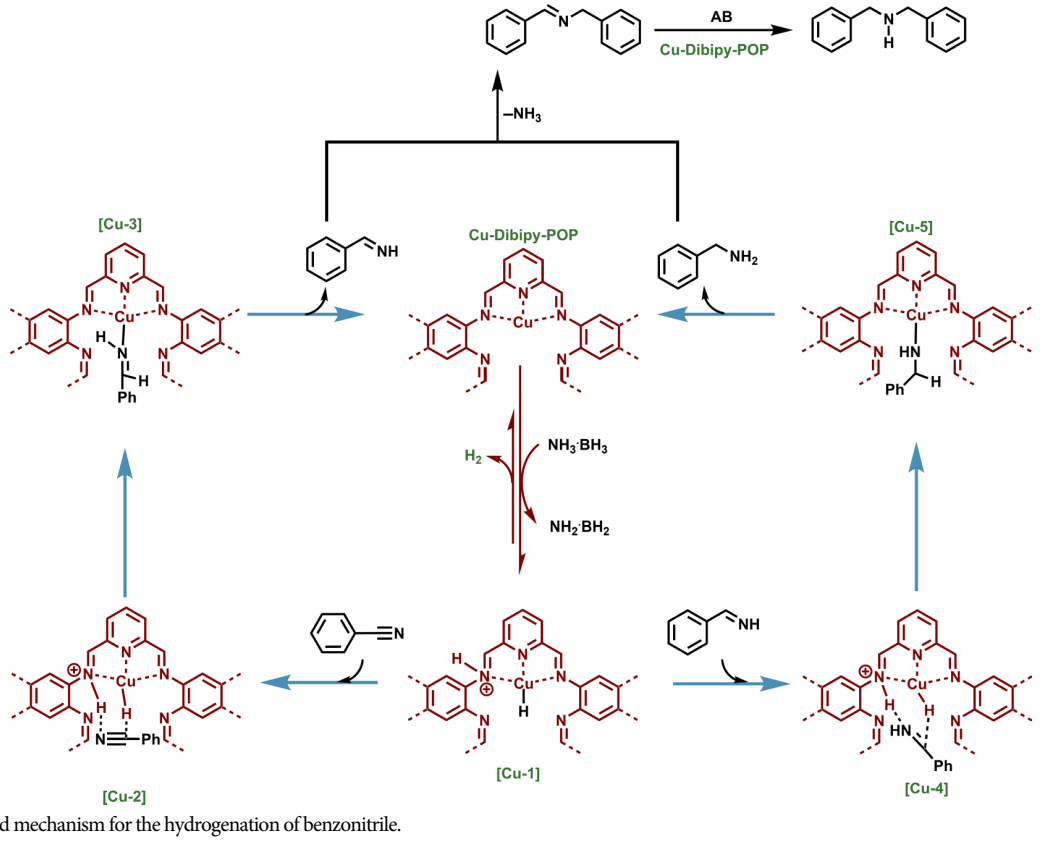

Figure 5 Proposed mechanism for the hydrogenation of benzonitrile.

gained considerable attention as a mild, efficient, and sustainable strategy. Therefore, we further evaluated the catalytic activity of **Cu-Dibipy-POP** for benzylamine dehydrogenation to prepare imine product [8, 63].

Under optimized conditions, the **Cu-Dibipy-POP** catalyst demonstrated excellent dehydrogenation activity toward benzylamine derivatives containing diverse electronic effects (electron-withdrawing and donating groups), steric hindrance, and substituent positions (Fig. 6). Five consecutive recycling experiments confirmed its recyclability and stability: the yield of N-benzylidene benzylamine remained between 98% and 94% (Fig. S17 in the ESM), confirming the catalyst's high efficiency and recyclability. FT-IR and XPS analyses were also performed to confirm the structural integrity of the **Cu-Dibipy-POP** after catalysis. FT-IR resluts indicated that the chemical skeleton of **Cu-Dibipy-POP** was maintained after the fifth catalytic dehydrogenation (Fig. S18 in the ESM). In contrast, a noticeable change in the copper valence distribution was observed following the dehydrogenation of benzylamine, where the proportion of Cu^{2+} species increased significantly (Fig. S19 in the ESM). This phenomenon can be attributed to the partial oxidation of Cu(I) species to Cu(II) during the catalytic dehydrogenation cycle. With increasing cycle numbers, the Cu(II) species progressively accumulate. Given that the Cu(II) species exhibit comparatively lower catalytic activity than the Cu(I) species for the dehydrogenation of benzylamine, the observed gradual decline in dehydrogenation yield over five consecutive recycling experiments can be reasonably explained.

To elucidate the dehydrogenation mechanism, a series of control experiments were systematically conducted. First, the blank control experiment (without catalyst) showed no imine product formation (Fig. S20(a) in the ESM), confirming the indispensable role of the catalyst. Subsequent catalytic tests using the metal-free **Dibipy-POP** skeleton gave only 12% imine product (Fig. S20(b) in the ESM), indicating that the POP material exhibits weak activity without metal ions. To exclude oxidative contributions from ambient oxygen, the reaction was performed under strict anaerobic conditions with **Cu-Dibipy-POP** (Fig. S20(c) in the ESM), revealing identical yields to aerobic conditions and confirming that molecular oxygen is not involved in the oxidation process. Notably, an alone $Cu(OAc)_2$ catalytic system achieved 35% yield (Fig. S20(d) in the ESM), demonstrating that Cu species act as the primary active sites, while the POP frameworks significantly enhance catalytic performance of $Cu(OAc)_2$ through the cooperative effect.

To further confirm the dehydrogenation capability of **Cu-Dibipy-POP** in this transformation, we conducted an experiment in which Pd/C-catalyzed hydrogenation of 2-vinylnaphthalene was performed using H_2 generated from the **Cu-Dibipy-POP**-catalyzed dehydrogenation of benzylamine. This reaction successfully drove the continuous hydrogenation of vinylnaphthalene to ethylnaphthalene with 80% yield, thereby verifying that **Cu-Dibipy-POP** enables hydrogen generation via catalyzing benzylamine dehydrogenation (Fig. S20(e) in the ESM) [10, 58].

As shown in Figs. S21(c) and S21(d) in the ESM, a comparative evaluation of the dehydrogenation of benzylamine was also conducted using copper(I) acetate and copper(II) acetate as benchmark catalysts. While both copper salts were capable of catalyzing the dehydrogenation of benzylamine to some extent, copper(I) acetate afforded a higher yield. Therefore, Cu(I) species are essential for the catalytic performance.

Based on control experiments, the reaction mechanism of **Cu-Dibipy-POP**-catalyzed benzylamine dehydrogenation is proposed as follows (Fig. 7): The nitrogen atom of the amino group in benzylamine initially coordinates to the Cu center, inducing β-H elimination to release the Cu–H species ([Cu-6]) and form an imine intermediate (Ph–CH=NH). Subsequently, the Cu–H species will convert to intermediate [Cu-7] under the effect of H_2O, following by the release of H_2 to regenerate catalyst **Cu-Dibipy-POP** and complete the catalytic cycle. Finally, benzylamine and imine intermediate yield N-benzylidene benzylamine through a condensation reaction.

Based on the aforementioned studies of hydrogenation and dehydrogenation transformations, we conducted a comprehensive mechanistic analysis of these two opposing chemical reactions. Mechanistically, both the hydrogenation of benzonitrile and the dehydrogenative conversion of benzylamine involve a common reaction step: hydride transfer mediated by a metal-hydride species. Therefore, the ability and efficiency of metal-hydride species in transferring hydride are critical to both reactions. In this study, the designed bipyridine-bisimine coordination unit provides strong

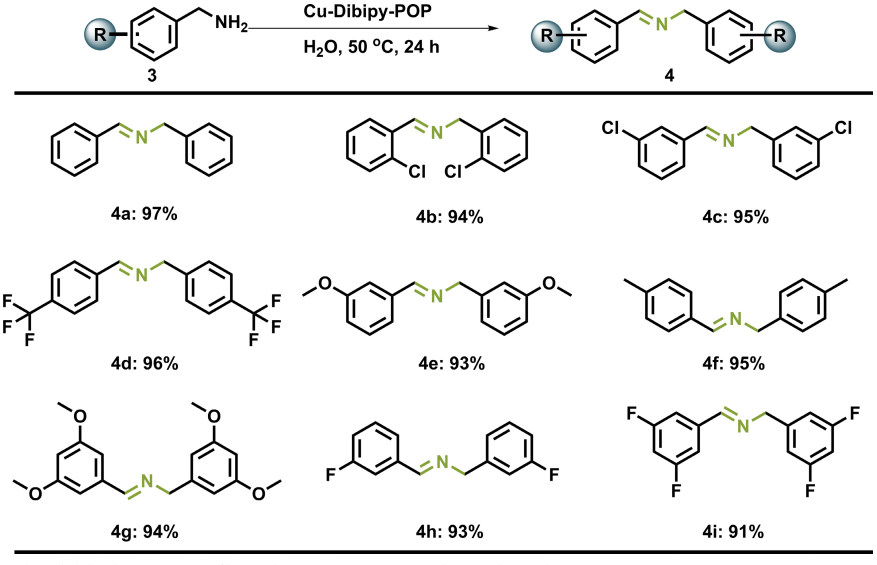

Figure 6 **Cu-Dibipy-POP**-catalyzed dehydrogenation of benzylamine. Reaction conditions: benzylamine (50 μL), **Cu-Dibipy-POP** (50 mg), solvent (5 mL), 50 °C, 24 h.

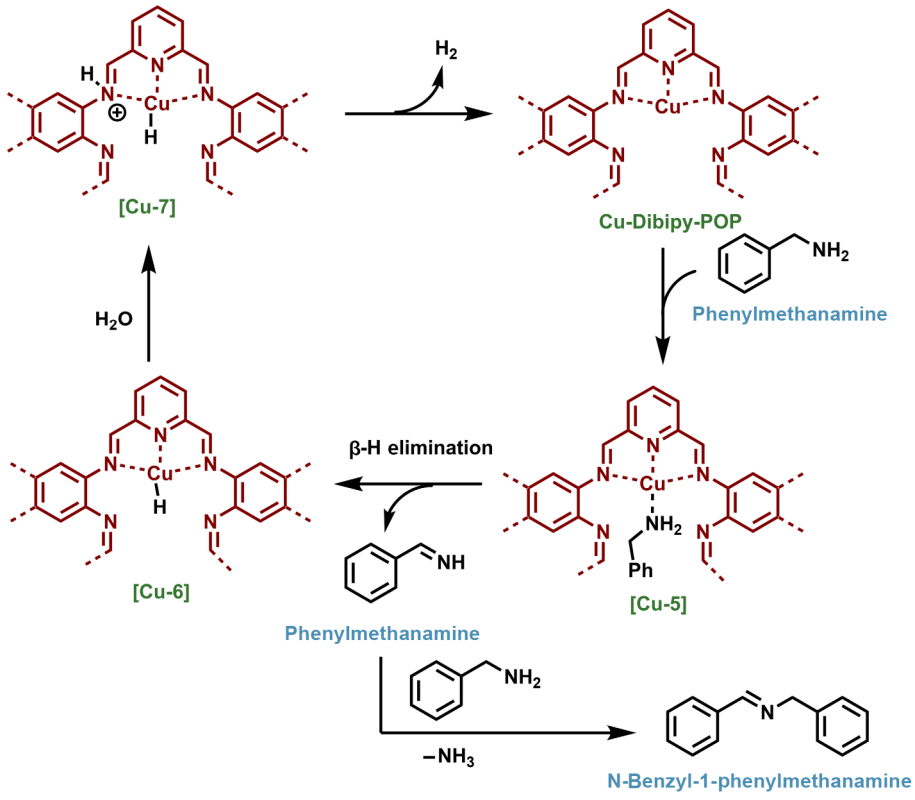

Figure 7 Proposed mechanism for the **Cu-Dibipy-POP** catalyzed dehydrogenation of benzylamine.

electron-donating effects to the metal center, facilitating M–H bond cleavage and enabling efficient hydride transfer. Furthermore, the pyridine-bisimine ligand is redox-active, capable of stabilizing low-valent metal species during the reaction, thereby creating a stable coordination environment for the monovalent copper-catalyzed hydrogenation of benzonitrile and the dehydrogenation pathway of benzylamine.

Another critical issue is that our initial surface area analysis of **Cu-Dibipy-POP** revealed a relatively low specific surface area and small pore size, which are theoretically anticipated to hinder mass transport of substrates and thus limit the catalytic efficiency. To elucidate whether the specific surface area of the catalytic material plays a significant role in the reaction, we employed the previously reported **Cu-Bipy-COF**—a material featuring a higher surface area and copper-coordinated bis(imino)pyridine units—as a catalyst for the hydrogenation of benzonitrile and dehydrogenation of benzylamine [44]. In contrast to our binuclear **Cu-Dibipy-POP**, **Cu-bipy-COF** exhibited significantly inferior catalytic performance, despite its substantially larger surface area (663.5 $m^2 \cdot g^{-1}$) and identical copper-coordinated ligand environment (Figs. S22 and S23 in the ESM). Therefore, despite **Cu-Dibipy-POP** shows low specific surface area, it exhibits exceptional catalytic activity, even surpassing catalyst with high surface areas. This superior performance is attributed to its redox-active dibis(imino)pyridine coordination structure, which effectively stabilizes low-valent copper active species. This result unambiguously confirms the unique advantage of the dibis(imino)pyridine motif design within the **Cu-Dibipy-POP** material.

3 Conclusions

In this study, we developed a novel POP incorporating dibis(imino)pyridine coordination units as macro-ligands for copper ions. This POP catalyst demonstrates exceptional activity for both benzylamine dehydrogenation and nitrile hydrogenation, encompassing three critical carbon nitrogen bond transformations: (1) C(sp^3)H–NH bond dehydrogenation, (2) C=N double bond hydrogenation, and (3) C≡N triple bond hydrogenation. These two catalytic systems were operated under sustainable conditions (aqueous medium, ≤ 80 °C) without noble metals, while maintaining consistent yields over multiple cycles. The electron-rich dibis(imino)pyridine framework could weak the strength of metal-hydride bond, enabling reversible hydrogen transfer with high efficiency. This work establishes a new paradigm for sustainable carbon nitrogen bond de/hydrogenation transformations through rational design of multifunctional POP catalysts, combining the precision of homogeneous catalysis with the practicality of heterogeneous systems.

Electronic Supplementary Material: Supplementary material (further details of the materials preparation methods and de/hydrogenation procedures, CP/MAS ^{13}C NMR spectroscopy, FT-IR, PXRD, SEM measurements, thermogravimetric curves, and XPS and UV–Vis spectroscopy measurements) is available in the online version of this article at https://doi.org/10.26599/NR.2026.94908329.

Data availability

All data needed to support the conclusions in the paper are presented in the manuscript and the Electronic Supplementary Material. Additional data related to this paper may be requested from the corresponding author upon request.

Acknowledgements

We are grateful for the financial support of the National Natural Science Foundation of China (No. 22202238) and Young Backbone Teacher of Zhongyuan University of Technology (No. 2024XQG01).

Declaration of competing interest

All the contributing authors report no conflict of interests in this work.

Author contribution statement

W. Y. A. and X. B. C.: Project administration, writing manuscript, experimental design. J. W. Z., L. D. L., J. X. D., W. Z. L., and J. Y. S.: Experimental design and practice. S. Y. W. and G. L. W.: Data curation, writing and revising manuscript.

Use of AI statement

None.

References

[1] Stevens, M. A.; Colebatch, A. L. Cooperative approaches in catalytic hydrogenation and dehydrogenation. *Chem. Soc. Rev.* **2022**, *51*, 1881–1898.

[2] Li, L. J.; He, Y. L.; Yang, Y. H.; Guo, J.; Lu, Z.; Wang, C. Y.; Zhu, S. L.; Zhu, S. F. Recent advances in Mn, Fe, Co, and Ni-catalyzed organic reactions. *CCS Chem.* **2024**, *6*, 537–584.

[3] Wang, Y.; Ma, F. Y.; Zhang, G. Q.; Zhang, J. W.; Zhao, H.; Dong, Y. M.; Wang, D. S. Precise synthesis of dual atom sites for electrocatalysis. *Nano Res.* **2024**, *17*, 9397–9427.

[4] Fan, Y. W.; Wang, P. X.; Zhang, J. H.; Huang, M. M.; Liu, W.; Xu, Y. L.; Duan, X. N.; Li, Y. Y.; Zhang, J. S. Continuous hydrogenation of N-ethylcarbazole in a micro-packed bed reactor for hydrogen storage. *Chem. Eng. J.* **2024**, *484*, 149404.

[5] Fan, Y. W.; Xu, Y. L.; Wang, P. X.; Liu, W.; Zhang, J. S. Continuous dehydrogenation of dodecahydro-N-ethylcarbazole for hydrogen production in a micro-packed bed reactor. *Int. J. Hydrogen Energy* **2025**, *103*, 787–796.

[6] Wang, B.; Li, P. Y.; Wang, S. Y.; Lu, S. H.; Fang, T. Tuning the interaction between Pd and $MgAl_2O_4$ to enhance the dehydrogenation activity and selectivity of dodecahydro-N-ethylcarbazole. *ACS Sustain. Chem. Eng.* **2023**, *11*, 5485–5494.

[7] Beaucage, N.; Singh, Z.; Bourdon, J.; Collins, S. K. Tuning co-operative energy transfer in copper(I) complexes using two-photon absorbing Diimine-based ligand sensitizers. *Angew. Chem., Int. Ed.* **2025**, *64*, e202412606.

[8] Qiao, Z. R.; Cao, H. Q.; Wang, J. D.; Yang, H. J.; Yao, W. Q.; Wang, J. O.; Cheetham, A. K. Curvature-induced electron spin catalysis with carbon spheres. *Angew. Chem., Int. Ed.* **2025**, *64*, e202412745.

[9] Wang, H. W.; Luo, Q. Q.; Liu, W.; Lin, Y.; Guan, Q. Q.; Zheng, X. S.; Pan, H. B.; Zhu, J. F.; Sun, Z. H.; Wei, S. Q. et al. Quasi Pd_1Ni single-atom surface alloy catalyst enables hydrogenation of nitriles to secondary amines. *Nat. Commun.* **2019**, *10*, 4998.

[10] Yamaguchi, R.; Ikeda, C.; Takahashi, Y.; Fujita, K. I. Homogeneous catalytic system for reversible dehydrogenation–hydrogenation reactions of nitrogen heterocycles with reversible interconversion of catalytic species. *J. Am. Chem. Soc.* **2009**, *131*, 8410–8412.

[11] Liu, Z. X.; Du, J.; Li, S.; Zhu, M. Q.; Ma, Y. Y.; Han, Z. G. Synergistic crystalline catalysts assembled with Wells-Dawson-type polyoxometalates and heterovalent metal complexes for efficient benzylic C–H bond oxidation. *Inorg. Chem. Front.* **2025**, *12*, 4078–4090.

[12] Li, S.; Han, Q.; Ma, Y. Y.; Zhang, S. M.; Du, J.; Han, Z. G. Polyoxometalate-encapsulated copper-organic complexes for efficient C–H bond oxidation of alkylbenzenes. *J. Mol. Struct.* **2025**, *1342*, 142686.

[13] He, J. Y.; Wang, J. F.; Du, J.; Ma, Y. Y.; Han, Z. G. *In situ* organic transformation reactions involved in synthesis process of polyoxometalate-based hybrids. *Eur. J. Inorg. Chem.* **2025**, *28*, e202400584.

[14] Tang, S.; Rauch, M.; Montag, M.; Diskin-Posner, Y.; Ben-David, Y.; Milstein, D. Catalytic oxidative deamination by water with H_2 liberation. *J. Am. Chem. Soc.* **2020**, *142*, 20875–20882.

[15] Patil, U. P. Porous carbon catalysis in sustainable synthesis of functional heterocycles: An overview. *Chin. Chem. Lett.* **2024**, *35*, 109472.

[16] Ito, H.; Mitamura, Y.; Segawa, Y.; Itami, K. Inside cover: Thiophene-based, radial π-conjugation: Synthesis, structure, and photophysical properties of cyclo-1,4-phenylene-2′,5′-thienylenes. *Angew. Chem., Int. Ed.* **2015**, *54*, 2.

[17] Shao, Z. H.; Fu, S. M.; Wei, M. F.; Zhou, S. L.; Liu, Q. Mild and selective cobalt-catalyzed chemodivergent transfer hydrogenation of nitriles. *Angew. Chem., Int. Ed.* **2016**, *55*, 14653–14657.

[18] Zhao, B. G.; Han, Z. B.; Ding, K. L. The N–H functional group in organometallic catalysis. *Angew. Chem., Int. Ed.* **2013**, *52*, 4744–4788.

[19] Kirichenko, O. A.; Kustov, L. M. Recent progress in development of supported palladium catalysts for dehydrogenation of heterocyclic liquid organic hydrogen carriers (LOHC). *Int. J. Hydrogen Energy* **2024**, *88*, 97–119.

[20] Zhou, M. J.; Miao, Y. L.; Gu, Y. W.; Xie, Y. J. Recent advances in reversible liquid organic hydrogen carrier systems: From hydrogen carriers to catalysts. *Adv. Mater.* **2024**, *36*, 2311355.

[21] Wang, X. Y.; Wei, W. J.; Zhou, S. Y.; Pan, Y. Z.; Yang, J. R.; Gan, T.; Zhuang, Z. C.; Li, W. H.; Zhang, X.; Pan, Y. M. et al. Phosphorus-doped single atom copper catalyst as a redox mediator in the cathodic reduction of quinazolinones. *Angew. Chem., Int. Ed.* **2025**, *64*, e202505085.

[22] Li, W. H.; Ye, B. C.; Yang, J. R.; Wang, Y.; Yang, C. J.; Pan, Y. M.; Tang, H. T.; Wang, D. S.; Li, Y. D. A single-atom cobalt catalyst for the fluorination of acyl chlorides at parts-per-million catalyst loading. *Angew. Chem., Int. Ed.* **2022**, *61*, e202209749.

[23] Wang, Y.; Liu, Q.; Ma, Y. Y.; Liu, Z. X.; Zhang, Y. N.; Wang, Y. S.; Du, J.; Han, Z. G. Polyoxometalate-embedded copper-organic network as dual-site synergetic catalyst for the selective oxidation of benzylic C–H bond. *Mol. Catal.* **2024**, *569*, 114579.

[24] Chen, X. Y.; Geng, K. Y.; Liu, R. Y.; Tan, K. T.; Gong, Y. F.; Li, Z. P.; Tao, S. S.; Jiang, Q. H.; Jiang, D. L. Covalent organic frameworks: Chemical approaches to designer structures and built-in functions. *Angew. Chem., Int. Ed.* **2020**, *59*, 5050–5091.

[25] Das, S.; Heasman, P.; Ben, T.; Qiu, S. L. Porous organic materials: Strategic design and structure–function correlation. *Chem. Rev.* **2017**, *117*, 1515–1563.

[26] Liu, X.; Liu, C. F.; Xu, S. H.; Cheng, T.; Wang, S.; Lai, W. Y.; Huang, W. Porous organic polymers for high-performance supercapacitors. *Chem. Soc. Rev.* **2022**, *51*, 3181–3225.

[27] Yang, D. H.; Tao, Y.; Ding, X. S.; Han, B. H. Porous organic polymers for electrocatalysis. *Chem. Soc. Rev.* **2022**, *51*, 761–791.

[28] Zhang, Z. W.; Jia, J.; Zhi, Y. F.; Ma, S.; Liu, X. M. Porous organic polymers for light-driven organic transformations. *Chem. Soc. Rev.* **2022**, *51*, 2444–2490.

[29] Wang, S. W.; Wang, L. G.; Zhou, X. D.; Fang, J. J.; Deng, C.; Wang, D. S. Design principles of single-atom catalysts anchored over porous materials for green catalysis and conversion. *Nano Res.* **2025**, *18*, 94907137.

[30] Kramer, S.; Bennedsen, N. R.; Kegnæs, S. Porous organic polymers containing active metal centers as catalysts for synthetic organic chemistry. *ACS Catal.* **2018**, *8*, 6961–6982.

[31] Ye, B. C.; Li, W. H.; Zhang, X.; Chen, J.; Gao, Y.; Wang, D. S.; Pan,

H. G. Advancing heterogeneous organic synthesis with coordination chemistry-empowered single-atom catalysts. *Adv. Mater.* **2024**, *36*, 2402747.

[32] Arora, V.; Yasmin, E.; Tanwar, N.; Hathwar, V. R.; Wagh, T.; Dhole, S.; Kumar, A. Pincer-ruthenium-catalyzed reforming of methanol-selective high-yield production of formic acid and hydrogen. *ACS Catal.* **2023**, *13*, 3605–3617.

[33] Duan, Y. Y.; Zhang, Y. K.; Cheng, Y. Z.; Bao, X. T.; Gao, K. F.; Huang, B. R.; Li, S. Q.; Bai, H. M.; Gong, Y.; Yang, D. H. et al. Construction of metal-N_3 sites in covalent organic frameworks for enhancing CO_2 photoreduction. *Appl. Catal. B: Environ. Energy* **2025**, *368*, 125117.

[34] Gibson, V. C.; Redshaw, C.; Solan, G. A. Bis(imino)pyridines: Surprisingly reactive ligands and a gateway to new families of catalysts. *Chem. Rev.* **2007**, *107*, 1745–1776.

[35] Li, Z. W.; Li, Y. N.; Cheng, H. J.; Song, Y. R.; Jiao, Y. Y.; Shi, S. B.; Gao, J. F.; Sun, L. C.; Hou, J. G. Atomically dispersed Ni active sites on covalent organic frameworks for heterogeneous metallaphotocatalytic C–N cross-coupling. *Appl. Catal. B: Environ. Energy* **2024**, *345*, 123698.

[36] Bart, S. C.; Chłopek, K.; Bill, E.; Bouwkamp, M. W.; Lobkovsky, E.; Neese, F.; Wieghardt, K.; Chirik, P. J. Electronic structure of bis(imino)pyridine iron dichloride, monochloride, and neutral ligand complexes: A combined structural, spectroscopic, and computational study. *J. Am. Chem. Soc.* **2006**, *128*, 13901–13912.

[37] Römelt, C.; Weyhermüller, T.; Wieghardt, K. Structural characteristics of redox-active pyridine-1,6-diimine complexes: Electronic structures and ligand oxidation levels. *Coordin. Chem. Rev.* **2019**, *380*, 287–317.

[38] Ai, W. Y.; Zhong, R.; Liu, X. F.; Liu, Q. Hydride transfer reactions catalyzed by cobalt complexes. *Chem. Rev.* **2019**, *119*, 2876–2953.

[39] Ai, W. Y.; Du, X.; Yang, Y.; Zheng, Z. L.; Zhai, L. P.; Ma, B. W.; Cui, S. W.; Li, P. Y.; Mi, L. W.; Qu, L. B. A metal-covalent organic framework catalyst with pincer coordination units for boosting transfer hydrogenation of quinolines with ammonia borane. *J. Mater. Chem. A* **2022**, *10*, 18602–18608.

[40] Qian, H. L.; Meng, F. L.; Yang, C. X.; Yan, X. P. Irreversible amide-linked covalent organic framework for selective and ultrafast gold recovery. *Angew. Chem., Int. Ed.* **2020**, *59*, 17607–17613.

[41] Ai, W. Y.; Zou, J. W.; Cao, Z. F.; Cui, K.; Gu, J. B.; Du, L. N.; Peng, X.; Jiao, M. L.; Shen, T.; Qu, L. B. Spontaneous conversion of pyridine N-oxide ylide covalent organic framework (COF) into biradical COF as an efficient catalyst in catalytic dehydrogenation of nitrogen heterocycles. *Chem. Sci.* **2025**, *16*, 12439–12448.

[42] Guo, L. J.; Gao, Y. X.; Huang, J.; Xue, J. Q.; Li, F.; Li, C. Q. Imine-linked covalent organic frameworks coordinated with nickel for ethylene oligomerization. *J. Appl. Polym. Sci.* **2023**, *140*, e53320.

[43] Li, Y.; Guo, X. H.; Li, X. F.; Zhang, M. C.; Jia, Z. M.; Deng, Y.; Tian, Y.; Li, S. J.; Ma, L. J. Redox-active two-dimensional covalent organic frameworks (COFs) for selective reductive separation of valence-variable, redox-sensitive and long-lived radionuclides. *Angew. Chem., Int. Ed.* **2020**, *59*, 4168–4175.

[44] Ai, W. Y.; Liu, Y.; Lan, Y. S.; Zou, J. W.; Cui, K.; Du, J. L.; Li, P. Y.; Yang, Y.; Gu, J. B.; Shen, T. et al. *In situ* reversible formation proton-shuttling covalent organic framework catalyst for promoting hydration of nitriles. *ACS Mater. Lett.* **2025**, *7*, 172–180.

[45] Zhang, Y.; Liu, Y. F.; Wang, D.; Liu, J. C.; Zhao, J. W.; Chen, L. J. State-of-the-art advances in the syntheses, structures, and applications of polyoxometalate-based metal-organic frameworks. *Polyoxometalates.* **2023**, *2*, 9140017.

[46] Ravel, B.; Newville, M. ATHENA, ARTEMIS, HEPHAESTUS: Data analysis for X-ray absorption spectroscopy using IFEFFIT. *J. Synchrotron Rad.* **2005**, *12*, 537–541.

[47] Srimani, D.; Feller, M.; Ben-David, Y.; Milstein, D. Catalytic coupling of nitriles with amines to selectively form imines under mild hydrogen pressure. *Chem. Commun.* **2012**, *48*, 11853–11855.

[48] Azizi, S.; Darroudi, M.; Soleymani, J.; Shadjou, N. $Tb_2(WO_4)_3$@N-GQDs-FA as an efficient nanocatalyst for the efficient synthesis of *β*-aminoalcohols in aqueous solution. *J. Mol. Liq.* **2021**, *329*, 115555.

[49] Zhou, Y.; Liu, Z. Q.; Yuan, T. T.; Huang, J. B.; Liu, C. J. The synthesis of 2-aminobenzoxazoles using reusable ionic liquid as a green catalyst under mild conditions. *Molecules* **2017**, *22*, 576.

[50] Lamani, M.; Prabhu, K. R. Iodine-catalyzed amination of benzoxazoles: A metal-free route to 2-aminobenzoxazoles under mild conditions. *J. Org. Chem.* **2011**, *76*, 7938–7944.

[51] Froehr, T.; Sindlinger, C. P.; Kloeckner, U.; Finkbeiner, P.; Nachtsheim, B. J. A metal-free amination of benzoxazoles-the first example of an iodide-catalyzed oxidative amination of heteroarenes. *Org. Lett.* **2011**, *13*, 3754–3757.

[52] Zhang, Y. C.; Li, P. H.; Wang, M.; Wang, L. Indium-catalyzed highly efficient three-component coupling of aldehyde, alkyne, and amine via C–H bond activation. *J. Org. Chem.* **2009**, *74*, 4364–4367.

[53] Bagal, D. B.; Bhanage, B. M. Recent advances in transition metal-catalyzed hydrogenation of nitriles. *Adv. Synth. Catal.* **2015**, *357*, 883–900.

[54] Chakraborty, S.; Berke, H. Homogeneous hydrogenation of nitriles catalyzed by molybdenum and tungsten amides. *ACS Catal.* **2014**, *4*, 2191–2194.

[55] Jiang, H.; Deng, D.; Kita, Y.; Hattori, M.; Kamata, K.; Hara, M. Tuning the selectivity of catalytic nitrile hydrogenation with phase-controlled co nanoparticles prepared by hydrosilane-assisted method. *J. Am. Chem. Soc.* **2024**, *146*, 20919–20929.

[56] Chatterjee, M.; Kawanami, H.; Sato, M.; Ishizaka, T.; Yokoyama, T.; Suzuki, T. Hydrogenation of nitrile in supercritical carbon dioxide: A tunable approach to amine selectivity. *Green Chem.* **2010**, *12*, 87–93.

[57] Lundevall, F. J.; Elumalai, V.; Drageset, A.; Totland, C.; Bjørsvik, H. R. A Co_2B mediated $NaBH_4$ reduction protocol applicable to a selection of functional groups in organic synthesis. *Eur. J. Org. Chem.* **2018**, *2018*, 3416–3425.

[58] Zhang, X. Y.; Zhang, J. H.; Hao, Z. Q.; Han, Z. G.; Lin, J.; Lu, G. L. Nickel complexes bearing N,N,O-tridentate salicylaldiminato ligand: Efficient catalysts for imines formation via dehydrogenative coupling of primary alcohols with amines. *Organometallics.* **2021**, *40*, 3843–3853.

[59] Huang, B.; Tian, H. W.; Lin, S. S.; Xie, M. H.; Yu, X. C.; Xu, Q. Cu(I)/TEMPO-catalyzed aerobic oxidative synthesis of imines directly from primary and secondary amines under ambient and neat conditions. *Tetrahedron Lett.* **2013**, *54*, 2861–2864.

[60] Liu, L. X.; Sun, H. L. $[HCo(CO)_4]$-catalyzed three-component cycloaddition of epoxides, imines, and carbon monoxide: Facile construction of 1,3-oxazinan-4-ones. *Angew. Chem. , Int. Ed.* **2014**, *53*, 9865–9869.

[61] McLaughlin, M.; Takahashi, M.; Micalizio, G. C. An alkoxide-directed intermolecular [2+2+1] annulation: A three-component coupling reaction for the synthesis of tetrasubstituted α,β-unsaturated γ-lactams. *Angew. Chem., Int. Ed.* **2007**, *46*, 3912–3914.

[62] Shiino, M.; Watanabe, Y.; Umezawa, K. Synthesis of *N*-substituted *N*-nitrosohydroxylamines as inhibitors of mushroom tyrosinase. *Bioorgan. Med. Chem.* **2001**, *9*, 1233–1240.

[63] Sun, Q. Y.; He, H. Z.; Zhou, Y.; Dai, Y. P.; Shang, P.; Jiang, X. F. Photocatalytic hydroxylation and oxidative coupling reactions mediated by multinuclear Au(I) supramolecular clusters. *Angew. Chem., Int. Ed.* **2025**, *64*, e202420499.